Proceedings of the 3rd International Symposium on Uncertainty Quantification and Stochastic Modeling
D.A. Rade; A. M. G. Lima (Editors), ABCM, Maresias, SP, Brazil, February 15-19, 2016

EFFECTS OF A RANDOM LOADING EMULATING AN IRREGULAR TERRAIN IN THE NONLINEAR DYNAMICS OF A TOWER SPRAYER

Americo Cunha Jr[1], Jorge Luis Palacios Felix[2], and José Manoel Balthazar[3]

[1] Universidade do Estado do Rio de Janeiro — americo.cunhajr@ime.uerj.br

[2] Universidade Federal do Pampa — jorge.felix@unipampa.edu.br

[3] Instituto Tecnológico de Aeronáutica — jmbaltha@ita.br

Abstract: This paper deals with the nonlinear dynamics of a mechanical system which consists of an orchard tower sprayer, coupled with a vehicle suspension that is subject to random excitations due to soil irregularities. A deterministic mathematical model, where tower is considered as an inverted double pendulum over an vehicle suspension, with three degrees of freedom (one translation and two rotations) is constructed. To take into account the random loadings due to soil variabilities, a parametric probabilistic approach is employed, where the external force is assumed to be a harmonic random process. This stochastic process has random amplitude and frequency, which are modeled as random variables, and a sinusoidal shape in time. The distribution of these random parameters is consistently specified using the maximum entropy principle. The propagation of uncertainties through the stochastic model is computed using the Monte Carlo method. Numerical simulations show large discrepancies in the system response, when compared with nominal (deterministic) model, for the cases studied where the forcing frequency is random. Also, the results shown that the steady state probability distributions are completely different in all the case studied.

Keywords: nonlinear dynamics; orchard tower sprayer; double inverted pendulum; uncertainty quantification; parametric probabilistic approach

1 INTRODUCTION

The process of spray orchards is of extreme importance in fruit growing, not only to prevent the economic damages associated with the loss of a production, but also to ensure the quality of the fruit that will arrive the final consumer. This process uses an equipment, called *tower sprayer*, which is illustrated in Figure 1. This equipment is composed by two main devices, a vehicle suspension and a support tower equipped with several fans, and in a typical operating condition, it vibrates nonlinearly (Sartori Junior *et al.*, 2009).

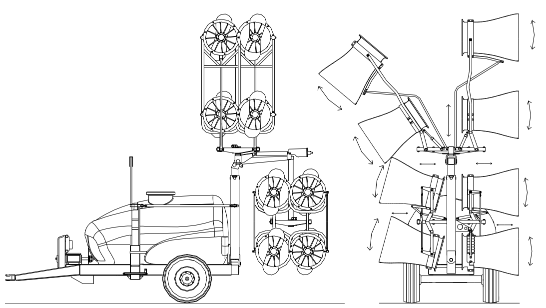

Figure 1 – Schematic representation of the tower sprayer. Adapted from Sartori Junior (2008), and courtesy of Máquinas Agrícolas Jacto S/A.

This nonlinear dynamical system has been studied before in Sartori Junior *et al.* (2007), Sartori Junior (2008) and Sartori Junior *et al.* (2009), using a model that considers an inverted double pendulum mounted on a vehicular suspension to emulate the equipment. These works perform parametric analyzes to investigate the influence of certain quantities in the model, for instance, stiffness, torsional damping, etc., and conclude that the developed model respond consistently in all cases it was tested.

However, all the previous studies were performed from a deterministic point of view, which is not the most realistic perspective to deal with a complex physical system like this, once it is subject to a series of uncertainties Soize (2012, 2013). These uncertainties are translated as variabilities in the model parameters and in epistemic uncertainties, that are intrinsically associated with the analyst ignorance on the physics of the problem. Take into account these uncertainties is already a common task in engineering, and can be seen, for instance, in the dynamics analysis of drillings (Cunha Jr *et al.*, 2015), bars (Cunha Jr and Sampaio, 2015), and (Perrin *et al.*, 2015) rails, to identify models of materials (Ritto and Nunes, 2015), to perform robust optimization (Beck *et al.*, 2015), etc.

In a first analysis, taking into account only the model parameters uncertainties, the source of randomness in the tower sprayer dynamics that seems most notoriously is the one associated with tires excitation. This because, during its operation, the structure typically move in extremely rough terrains. Therefore, it is more realistic consider a stochastic model to describe the dynamic behavior of this physical system when subject to a random excitation in the tires. A first initiative in this direction was made in Cunha Jr *et al.* (2015), which presents the construction of a consistent stochastic model to describe the tower sprayer nonlinear dynamics. This work aims to continue this study, investigating in depth the effects induced by the tires random excitation in the tower sprayer response.

The rest of this paper is organized as follows. In section 2 it is presented the definition of the mechanical system and a deterministic model to describe its nonlinear dynamics. A stochastic model to to take into account the uncertainties associated to the model parameters is shown in section 3. The results of the numerical experiments conducted in this work are presented and discussed in section 4. Finally, in section 5, the main conclusions are highlighted.

2 DETERMINISTIC MODEL

This paper uses the model developed by Sartori Junior (2008); Sartori Junior *et al.* (2009), where the mechanical system is considered an inverted double pendulum, mounted on a vehicular suspension, as shown in Figure 2. The masses of the chassis and the tank are assumed to be concentrated at the bottom of the double pendulum, as a point mass denoted by m_1. On the other hand, the point mass m_2, at the top of the double pendulum, take into account the masses of the fans. The point of articulation between the moving suspension and the tower is denoted by P and its distance to the suspension center of gravity is L_1. The junction P has torsional stiffness k_T, and damping torsional coefficient c_T. The tower has length L_2, and is considered to be massless. The left wheel of the vehicle suspension is represented by a pair spring/damper with constant respectively given by k_1 and c_1, it is located at a distance B_1 from suspension center line, and it is subject to a vertical displacement y_{e1}. Similarly, the right wheel is represented by a pair spring/damper characterized by k_2 and c_2, it is B_2 away from suspension center line, and and displaces vertically y_{e2}. The moments of inertia of the suspension and of the tower, with respect to their centers of gravity, are respectively denoted by I_1 and I_2. Finally, introducing the inertial frame of reference XY, the vertical displacement of the suspension is measured by y_1, while its rotation is computed by ϕ_1, and the rotation of the tower is denoted by ϕ_2.

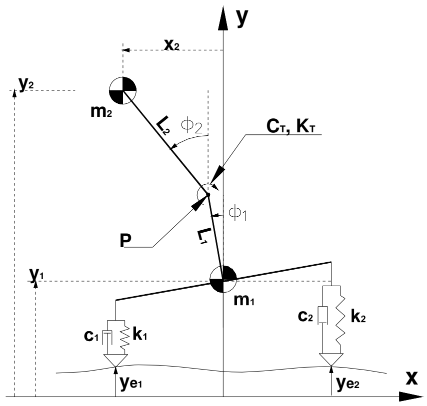

Figure 2 – Schematic representation of the mechanical-mathematical model: an inverted double pendulum, mounted on a moving suspension. Adapted from Sartori Junior (2008).

The left and right tires displacements are respectively assumed to be periodic functions in time, out of phase, with the same amplitude, and a single frequencial component,

$$y_{e1}(t) = A\,\sin\left(\omega\,t\right), \quad \text{and} \quad y_{e2}(t) = A\,\sin\left(\omega\,t + \rho\right), \tag{1}$$

where A and ω respectively denote the amplitude and frequency of the tires displacements, and ρ is the phase shift between the two tires.

The following ODE system describes the nonlinear dynamics of interest (Sartori Junior *et al.*, 2009)

$$[M] \begin{pmatrix} \ddot{y}_1(t) \\ \ddot{\phi}_1(t) \\ \ddot{\phi}_2(t) \end{pmatrix} + [N] \begin{pmatrix} \dot{y}_1^2(t) \\ \dot{\phi}_1^2(t) \\ \dot{\phi}_2^2(t) \end{pmatrix} + [C] \begin{pmatrix} \dot{y}_1(t) \\ \dot{\phi}_1(t) \\ \dot{\phi}_2(t) \end{pmatrix} + [K] \begin{pmatrix} y_1(t) \\ \phi_1(t) \\ \phi_2(t) \end{pmatrix} = \boldsymbol{g} - \boldsymbol{h}, \tag{2}$$

where $[M]$, $[N]$, $[C]$ and $[N]$ are 3×3 (configuration dependent) real matrices, respectively, defined by

$$[M] = \begin{bmatrix} m_1 + m_2 & -m_2\,L_1\,\sin\phi_1 & -m_2\,L_2\,\sin\phi_1 \\ -m_2\,L_1\,\sin\phi_1 & I_1 + m_2\,L_1^2 & m_2\,L_1\,L_2\,\cos\left(\phi_2 - \phi_1\right) \\ -m_2\,L_2\,\sin\phi_1 & m_2\,L_1\,L_2\,\cos\left(\phi_2 - \phi_1\right) & I_2 + m_2\,L_2^2 \end{bmatrix}, \tag{3}$$

$$[N] = \begin{bmatrix} 0 & -m_2\,L_1\,\cos\phi_1 & -m_2\,L_2\,\cos\phi_2 \\ 0 & 0 & -m_2\,L_1\,L_2\,\sin\left(\phi_2 - \phi_1\right) \\ 0 & -m_2\,L_1\,L_2\,\sin\left(\phi_2 - \phi_1\right) & 0 \end{bmatrix}, \tag{4}$$

$$[C] = \begin{bmatrix} c_1 + c_2 & (c_2\,B_2 - c_1\,B_1)\cos\phi_1 & 0 \\ (c_2\,B_2 - c_1\,B1)\cos\phi_1 & c_T + (c_1\,B_1^2 + c_2\,B_2^2)\cos^2\phi_1 & -c_T \\ 0 & -c_T & c_T \end{bmatrix}, \tag{5}$$

and

$$[K] = \begin{bmatrix} k_1 + k_2 & 0 & 0 \\ (k_2\,B_2 - k_1\,B1)\cos\phi_1 & k_T & -k_T \\ 0 & -k_T & k_T \end{bmatrix}, \tag{6}$$

and let $\boldsymbol{g}$, and $\boldsymbol{h}$ be (configuration dependent) vectors in $\mathbb{R}^3$, respectively, defined by

$$\boldsymbol{g} = \begin{pmatrix} (k_2\,B_2 - k_1\,B_1)\sin\phi_1 + (m_1 + m_2)g \\ (k_1\,B_1^2 + k_2\,B_2^2)\sin\phi_1\,\cos\phi_1 - m_2\,g\,L_1\,\sin\phi_1 \\ -m_2\,g\,L_2\,\sin\phi_2 \end{pmatrix}, \tag{7}$$

and

$$\boldsymbol{h} = \begin{pmatrix} k_1\,y_{e1} + k_2\,y_{e2} + c_1\,\dot{y}_{e1} + c_2\,\dot{y}_{e2} \\ -k_1\,B_1\,\cos\phi_1\,y_{e1} + k_2\,B_2\,\cos\phi_1\,y_{e2} - c_1\,B_2\,\cos\phi_1\,\dot{y}_{e1} + c_2\,B_2\,\cos\phi_1\,\dot{y}_{e2} \\ 0 \end{pmatrix}. \tag{8}$$

The nonlinear initial value problem, which is obtained when appropriate initial conditions are associated to the ODE system, is integrated using `ode45` routine from MATLAB (Shampine and Reichelt, 1997).

3 STOCHASTIC MODEL

The stochastic model is constructed in a probability space $(\Theta, \Sigma, \mathbb{P})$, being Θ the sample space, Σ a σ-field over Θ, and $\mathbb{P} : \Sigma \to [0,1]$ the probability measure. In this stochastic framework, the amplitude A, and the frequency ω are assumed as random parameters, being modeled by the random variables $\mathbb{A} : \Sigma \to \mathbb{R}$ and $\mathbb{w} : \Sigma \to \mathbb{R}$.

To specify the distribution of these random parameters, based only on theoretical information known about them, the maximum entropy principle is employed (Jaynes, 1957; Soize, 2013). For $\mathbb{A}$, that is a positive parameter, it is assumed that: (i) the support of the probability density function (PDF) is the positive real line, i.e., $\texttt{Supp}\, p_{\mathbb{A}} = (0, +\infty)$; and (ii) the mean value is known, i.e. $\mathbb{E}\left[\mathbb{A}\right] = \mu_{\mathbb{A}} \in (0, +\infty)$. Besides that, for $\mathbb{w}$, that is also a positive parameter, the only known information is assumed to be the support $\texttt{Supp}\, p_{\mathbb{w}} = [\omega_1, \omega_2] \subset (0, +\infty)$.

Consequently, the distributions which maximize the entropy have the following PDFs

$$p_{\mathbb{A}}(a) = \mathbb{1}_{(0,+\infty)}(a)\, \frac{1}{\mu_{\mathbb{A}}}\, \exp\left(-\frac{a}{\mu_{\mathbb{A}}}\right), \tag{9}$$

and

$$p_{\mathbb{w}}(\omega) = \mathbb{1}_{[\omega_1,\omega_2]}(\omega)\, \frac{1}{\omega_2 - \omega_1}, \tag{10}$$

which correspond, respectively, to the exponential and uniform distributions. In the above equations $\mathbb{1}_X(x)$ denotes the indicator function of the set X. Note that in Cunha Jr *et al.* (2015), the information that has been assumed about A and ω lead, respectively, to the gamma and beta distributions. A reflection, a posteriori, led the authors to conclude that the above choices are more consistent (as they are made based on less theoretical assumptions).

Due to the randomness of $\mathbb{A}$ and $\mathbb{w}$, the tire displacements are now described by the following random processes

$$\mathbb{y}_{e1}(t,\theta) = \mathbb{A}\, \sin\left(\mathbb{w}\, t\right), \quad \text{and} \quad \mathbb{y}_{e2}(t,\theta) = \mathbb{A}\, \sin\left(\mathbb{w}\, t + \rho\right). \tag{11}$$

Therefore, the dynamics of the mechanical system evolves (almost sure) according to the following system of stochastic differential equations

$$[M] \begin{pmatrix} \ddot{\mathbb{y}}_1(t,\theta) \\ \ddot{\phi}_1(t,\theta) \\ \ddot{\phi}_2(t,\theta) \end{pmatrix} + [N] \begin{pmatrix} \dot{\mathbb{y}}_1^2(t,\theta) \\ \dot{\phi}_1^2(t,\theta) \\ \dot{\phi}_2^2(t,\theta) \end{pmatrix} + [C] \begin{pmatrix} \dot{\mathbb{y}}_1(t,\theta) \\ \dot{\phi}_1(t,\theta) \\ \dot{\phi}_2(t,\theta) \end{pmatrix} + [K] \begin{pmatrix} \mathbb{y}_1(t,\theta) \\ \phi_1(t,\theta) \\ \phi_2(t,\theta) \end{pmatrix} = \boldsymbol{g} - \boldsymbol{h}. \quad a.s. \tag{12}$$

To compute the propagation of uncertainties of the random parameters through the nonlinear dynamics, it is employed the Monte Carlo (MC) method (Kroese *et al.*, 2011; Cunha Jr *et al.*, 2014).

4 NUMERICAL EXPERIMENTS

The nominal (deterministic) parameters presented in Table 1 are adopted to simulate the nonlinear dynamics of the mechanical system. For simplicity, all the initial conditions are assumed to be zero. The evolution of this nonlinear dynamic system is investigated for a "temporal window" defined by the interval $[t_0, t_f] = [0, 3] \times 10^2\ s$, using an adaptive time step, which is refined whenever necessary to capture the nonlinear effects.

Three stochastic experiments are considered. The first (case 1) considers only A as the random parameter. In the second (case 2), the random parameter is ω. In the final experiment (case 3), both A and ω are random. For the random variables $\mathbb{A}$ and $\mathbb{w}$, the parameters which define these random objects are $\mu_{\mathbb{A}} = 100 \times 10^{-3}\ m$, and $[\omega_1, \omega_2] = [1, 10]\ rad/s$.

Table 1 – Nominal (deterministic) parameters for the mechanical system that are used in the simulations.

parameter	value	unit
m_1	6500	kg
m_2	800	kg
L_1	200×10^{-3}	m
L_2	2400×10^{-3}	m
I_1	6850	$kg\, m^2$
I_2	6250	$kg\, m^2$
k_1	465×10^3	N/m
k_2	465×10^3	N/m
c_1	5.6×10^3	$N/m/s$
c_2	5.6×10^3	$N/m/s$
B_1	850×10^{-3}	m
B_2	850×10^{-3}	m
k_T	45×10^3	N/rad
c_T	50×10^3	$Nm/rad/s$
ρ	$\pi/9$	rad

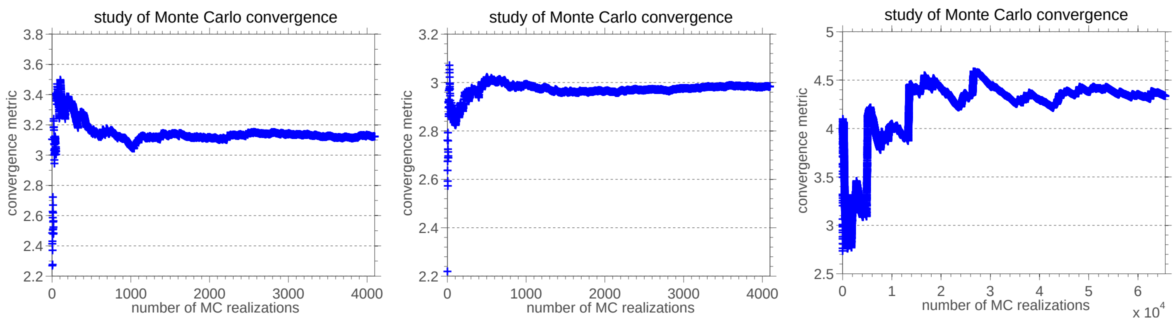

(a) case 1: A is random (b) case 2: ω is random (c) case 3: A and ω are random

Figure 3 – Illustration of MC convergence metric as function of the number of realizations.

4.1 Study of convergence for MC simulation

To evaluate the convergence of MC simulations, this work uses the map $n_s \in \mathbb{N} \mapsto \texttt{conv}(n_s) \in \mathbb{R}$, defined by

$$\texttt{conv}(n_s) = \left(\frac{1}{n_s} \sum_{n=1}^{n_s} \int_{t=t_0}^{t_f} \left(\mathbb{y}_1(t,\theta_n)^2 + \mathbb{\phi}_1(t,\theta_n)^2 + \mathbb{\phi}_2(t,\theta_n)^2 \right) \, dt \right)^{1/2}, \tag{13}$$

where n_s is the number of MC realizations. As shown in Soize (2005), this map allows one to evaluate the convergence of the approximation $\big(\mathbb{y}_1(t,\theta_n), \mathbb{\phi}_1(t,\theta_n), \mathbb{\phi}_2(t,\theta_n)\big)^T$ in the mean-square sense.

The evolution of $\texttt{conv}(n_s)$ as a function of n_s can be seen in Figure 3. Note that for $n_s = 4096$ the metric value has reached a steady value in all cases 1 and 2. On the other hand, in case 3, which has two random parameters, $n_s = 65536$ realizations were required to achieve statistical convergence.

4.2 Propagation of uncertainties through the nonlinear dynamics

In Figure 4 it is presented the evolution of suspension stochastic displacement for all cases analyzed. At this Figure, on the left, are represented the mean value (blue line), the nominal value (red line), and an envelope of reliability (grey shadow), wherein a realization of the stochastic system has 90% of probability of being contained. On the right the reader can see, on an enlarged scale, the mean and nominal values. Similar graphs can be seen in Figures 5 and 6, which respectively show, for all cases analyzed, the evolution of suspension stochastic rotation, and of the tower stochastic rotation.

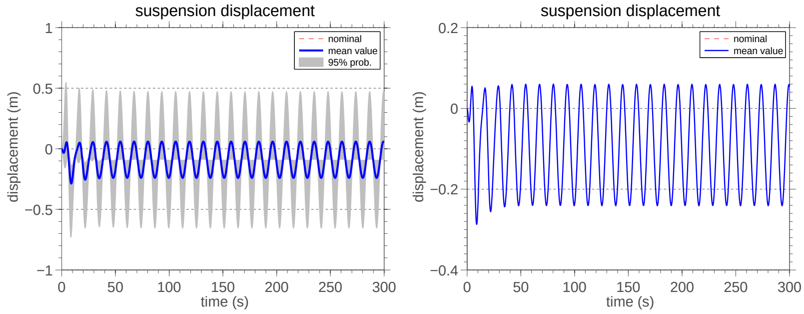

(a) case 1: A is random

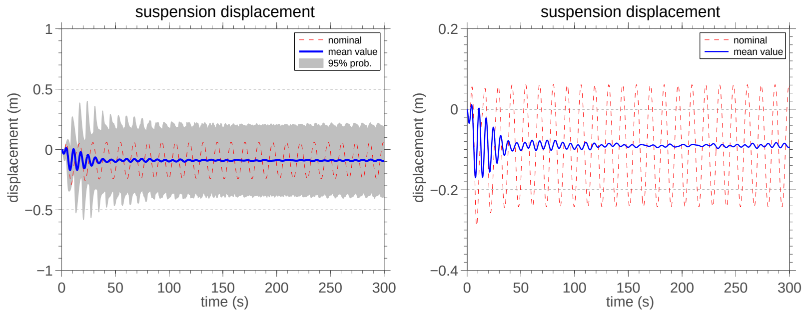

(b) case 2: ω is random

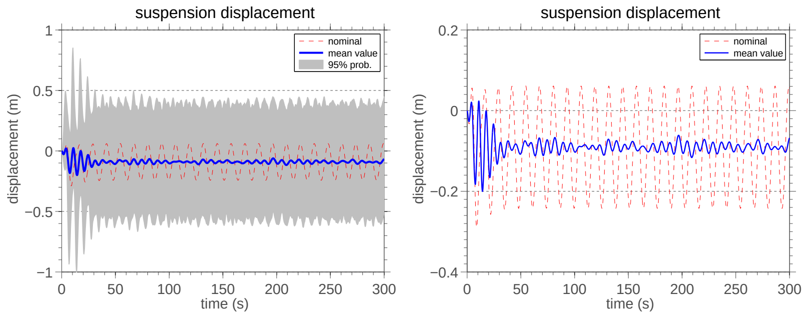

(c) case 3: A and ω are random

Figure 4 – This figure illustrates evolution of suspension translational dynamics. It can be seen the mean value (blue line), the nominal value (red line), and a 90% of probability confidence band (grey shadow).

Observing Figures 4 to 6 it can be noted that, in case 1 (uncertainty in A), the nominal model and the mean value of the system response are very close, and the band of reliability has a sinusoidal shape in phase with the response, with amplitude much larger than the nominal model amplitude. Beyond that, in Figure 6 one can observe a major tendency to have negative values in tower rotation, which, in principle, leads the structure to a stable configuration. Among the cases analyzed, this is the one with the lowest level of uncertainty.

In contrast, in case 2 (uncertainty in ω), the level of uncertainty observed is much more pronounced. Not only the mean value of the system response is completely different from the nominal model, as the band of reliability has larger area, with amplitude of comparable size or slightly bigger than the nominal model amplitude. Also, in this case, the system response mean value (at steady state) has not a purely sinusoidal appearance, because the system is forced at various frequencies.

The case 3 (uncertainty in A and ω) is the one with the highest level of uncertainty, which is not surprising, since it has two random parameters. Such as in case 2, there is great discrepancy between the mean value of the system response and the nominal model. But now the band of reliability amplitude is always much higher than the amplitude of the nominal model.

4.3 Probability distribution of the system response

The three degrees of freedom of the system response are the random processes $\mathbb{y}_1(t,\theta)$, $\mathbb{\phi}_1(t,\theta)$, and $\mathbb{\phi}_2(t,\theta)$. Computing the time average of these random processes, at the steady state, one obtains the random variables $< \mathbb{y}_1 >$, $< \mathbb{\phi}_1 >$, and $< \mathbb{\phi}_2 >$, each one with an underlying probability distribution. Accordingly, in what follows it is presented an analysis of the (normalized) probability density functions (PDFs) associated with the

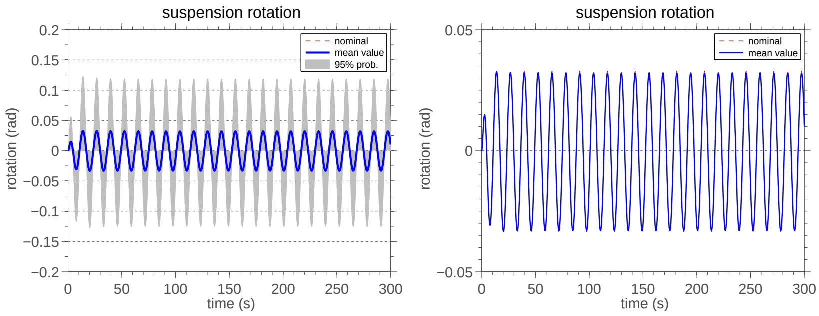

(a) case 1: A is random

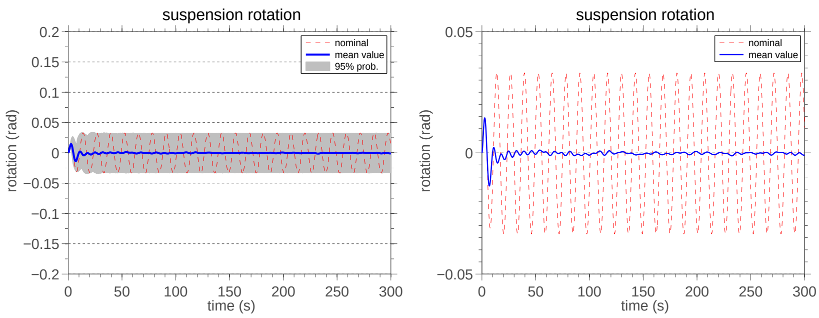

(b) case 2: ω is random

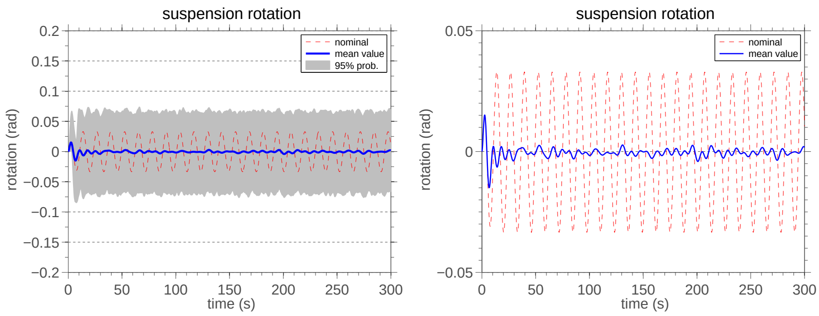

(c) case 3: A and ω are random

Figure 5 – This figure illustrates evolution of suspension rotational dynamics. It can be seen the mean value (blue line), the nominal value (red line), and a 90% of probability confidence band (grey shadow).

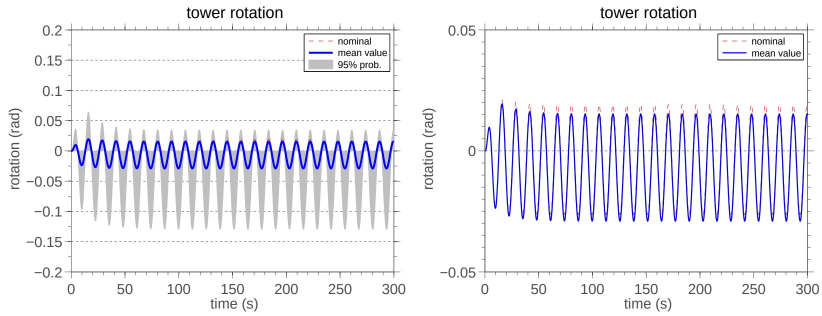

(a) case 1: A is random

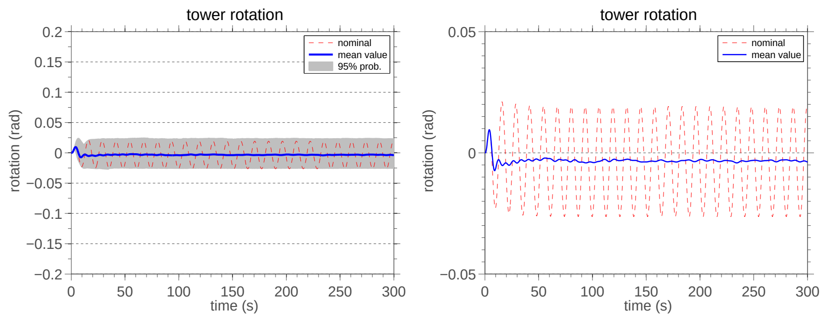

(b) case 2: ω is random

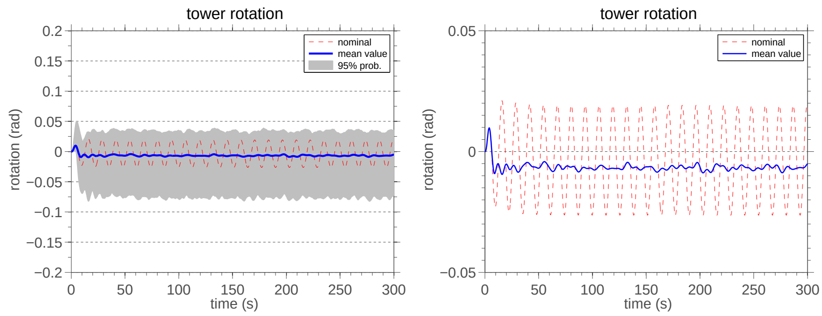

(c) case 3: A and ω are random

Figure 6 – This figure illustrates evolution of tower rotational dynamics. It can be seen the mean value (blue line), the nominal value (red line), and a 90% of probability confidence band (grey shadow).

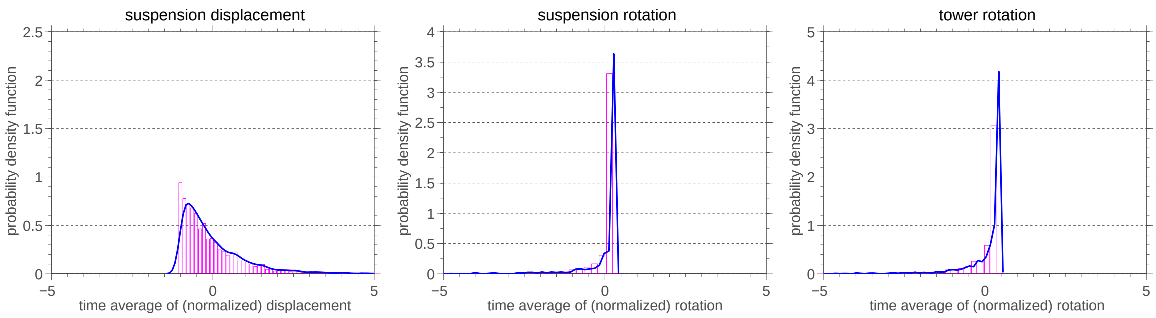

(a) case 1: A is random

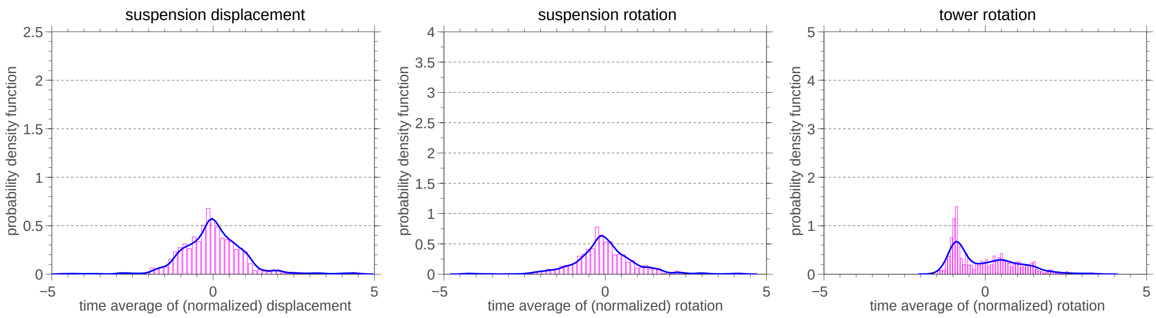

(b) case 2: ω is random

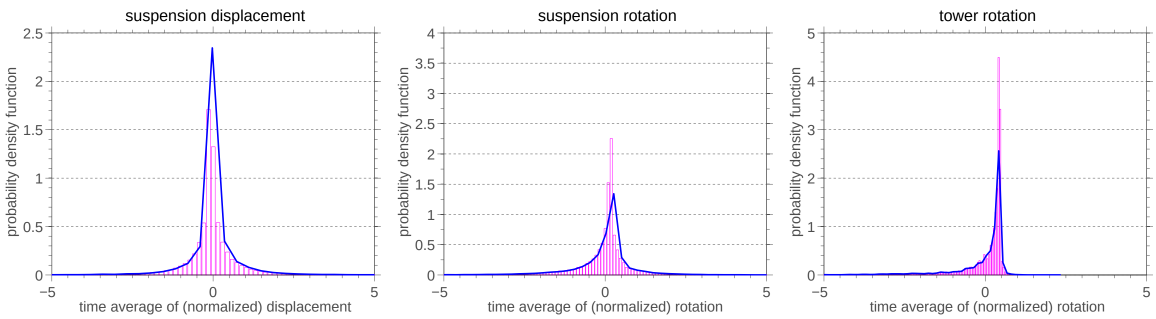

(c) case 3: A and ω are random

Figure 7 – This figure presents estimations to the (normalized) PDFs of time averaged suspension displacement (left), suspension rotation (middle), and tower rotation (right).

mechanical system response. In this context normalized means a random variable with zero mean and unit standard deviation.

In Figure 7, one can observe estimations for the (normalized) PDFs of the time average: (i) suspension displacement, (ii) suspension rotation, and (iii) tower rotation. Completely different behaviors are observed in the different cases analyzed. In the first case it is possible to observe large asymmetries with respect to the mean value, while in the second case the PDFs are almost symmetrical, except by the tower rotation, which, in addition to an asymmetry, presents bimodal behavior. In case 3 who presents a different behavior is, again, the tower rotation. Comparing also the PDF shape of a same random variable, among the different cases studied, one can also observe different behaviors.

5 FINAL REMARKS

This work presented the study of the nonlinear dynamics of an orchard tower sprayer, coupled with a vehicle suspension, that is subject to random excitations due to soil irregularities, modeled as an inverted double pendulum over a moving suspension, with three degrees of freedom (one translation and two rotations). The random loadings are take into account through a parametric probabilistic approach, where the external force was assumed to be a harmonic random process with random amplitude and frequency. The probability distribution of these random parameters was constructed using the maximum entropy principle. For the cases studied where the forcing frequency is random, the results of numerical simulation show large discrepancies in the stochastic system response compared nominal (deterministic) model. Furthermore, an analysis of the steady state probability distributions shows different behaviors in all the case studied.

6 ACKNOWLEDGMENTS

The authors are indebted to Brazilian agencies CNPq, CAPES, FAPERJ, FAPERGS, and FAPESP for the financial support given to this research. They are also grateful to Máquinas Agrícolas Jacto S/A for the important data supplied.

7 REFERENCES

Beck, A.T., Gomes, W.J.S., Lopez, R.H. and Miguel, L.F.F., 2015. "A comparison between robust and risk-based optimization under uncertainty". *Structural and Multidisciplinary Optimization*, Vol. 52, pp. 479–492. doi:10.1007/s00158-015-1253-9.

Cunha Jr, A., Felix, J.L.P. and Balthazar, J.M., 2015. "On the nonlinear dynamics of an inverted double pendulum over a vehicle suspension subject to random excitations". In *Proceedings of COBEM 2015*.

Cunha Jr, A., Nasser, R., Sampaio, R., Lopes, H. and Breitman, K., 2014. "Uncertainty quantification through Monte Carlo method in a cloud computing setting". *Computer Physics Communications*, Vol. 185, pp. 1355––1363. doi:10.1016/j.cpc.2014.01.006.

Cunha Jr, A. and Sampaio, R., 2015. "On the nonlinear stochastic dynamics of a continuous system with discrete attached elements". *Applied Mathematical Modelling*, Vol. 39, pp. 809—-819. doi:10.1016/j.apm.2014.07.012.

Cunha Jr, A., Soize, C. and Sampaio, R., 2015. "Computational modeling of the nonlinear stochastic dynamics of horizontal drillstrings". *Computational Mechanics*, pp. 849–878. doi:10.1007/s00466-015-1206-6.

Jaynes, E.T., 1957. "Information theory and statistical mechanics". *Physical Review Series II*, Vol. 106, pp. 620–630. doi:10.1103/PhysRev.106.620.

Kroese, D.P., Taimre, T. and Botev, Z.I., 2011. *Handbook of Monte Carlo Methods*. Wiley, New Jersey.

Perrin, G., Duhamel, D., Soize, C. and Funfschilling, C., 2015. "Quantification of the influence of the track geometry variability on the train dynamics". *Mechanical Systems and Signal Processing*, Vol. 60, pp. 945–957. doi:10.1016/j.ymssp.2015.01.004.

Ritto, T.G. and Nunes, L.C.S., 2015. "Bayesian model selection of hyperelastic models for simple and pure shear at large deformations". *Computers & Structures*, Vol. 156, pp. 101–109. doi:10.1016/j.compstruc.2015.04.008.

Sartori Junior, S., 2008. *Mathematical Modeling and Dynamic Analysis of a Orchards Spray Tower*. M.Sc. Dissertation, Universidade Estadual Paulista Julio de Mesquita Filho, Bauru. (in portuguese).

Sartori Junior, S., Balthazar, J.M. and Pontes Junior, B.R., 2009. "Non-linear dynamics of a tower orchard sprayer based on an inverted pendulum model". *Biosystems Engineering*, Vol. 103, pp. 417–426. doi:10.1016/j.biosystemseng.2008.09.003.

Sartori Junior, S., Balthazar, M. and Pontes, B.R., 2007. "Nonlinear dynamics of an orchard tower sprayer based on a double inverted pendulum model". In *Proceedings of COBEM 2007*.

Shampine, L.F. and Reichelt, M.W., 1997. "The MATLAB ODE Suite". *SIAM Journal on Scientific Computing*, Vol. 18, pp. 1–22. doi:10.1137/S1064827594276424.

Soize, C., 2005. "A comprehensive overview of a non-parametric probabilistic approach of model uncertainties for predictive models in structural dynamics". *Journal of Sound and Vibration*, Vol. 288, pp. 623–652. doi:10.1016/j.jsv.2005.07.009.

Soize, C., 2012. *Stochastic Models of Uncertainties in Computational Mechanics*. Amer Society of Civil Engineers, Reston.

Soize, C., 2013. "Stochastic modeling of uncertainties in computational structural dynamics — recent theoretical advances". *Journal of Sound and Vibration*, Vol. 332, pp. 2379—2395. doi:10.1016/j.jsv.2011.10.010.

RESPONSIBILITY NOTICE

The authors are the only responsible for the printed material included in this paper.